Biotechnology Reports 46 (2025) e00891

Contents lists available at ScienceDirect

Biotechnology Reports

journal homepage: www.elsevier.com/locate/btre

Montbretia flowers as a source of bioactive crocins: Biotechnology tools and delivery systems

Lucía Morote [a,1], Cristian Martínez Martínez Fajardo [a,1], María Mondéjar López [a], Elena Moreno-Gimenez [a], Ángela Rubio-Moraga [a,b], Olivia Costantina Demurtas [c], Gianfranco Diretto [c], Enrique Niza [a,d], Verónica Aragonés [e], Alberto López Jiménez [a,b], José-Antonio Daròs [e], Oussama Ahrazem [a,b], Lourdes Gómez-Gómez [a,d,*]

[a] Instituto Botánico. Departamento de Ciencia y Tecnología Agroforestal y Genética. Universidad de Castilla-La Mancha, Campus Universitario s/n, 02071 Albacete, Spain
[b] Escuela Técnica Superior de Ingenieros Agrónomos, Montes y Biotecnología. Departamento de Ciencia y Tecnología Agroforestal y Genética. Universidad de Castilla-La Mancha, Campus Universitario s/n, 02071 Albacete, Spain
[c] Italian National Agency for New Technologies, Energy, and Sustainable Development, Casaccia Research Centre, 00123 Rome, Italy
[d] Facultad de Farmacia, Departamento de Ciencia y Tecnología Agroforestal y Genética, Universidad de Castilla-La Mancha, Campus Universitario s/n, 02071 Albacete, Spain
[e] Instituto de Biología Molecular y Celular de Plantas (Consejo Superior de Investigaciones Científicas-Universitat Politècnica de València), 46022 Valencia, Spain

ARTICLE INFO

Keywords:
CCD
Crocin
Crocosmia x crocosmiiflora
Exosomes
Inflammation
Liposomes
Plant specialized metabolism

ABSTRACT

Crocins are potent antioxidants with significant therapeutic potential, exhibiting anti-inflammatory, anticancer, and antidepressant properties. The ornamental plant *Crocos-mia x crocosmiiflora* is widely cultivated for its aromatic and vibrant flowers. In this study, we identified unique crocins as the primary pigments responsible for the flower's coloration. These metabolites predominantly consist of molecules with eight glucose units, followed by crocins containing six and seven glucose units. To elucidate the mo-lecular mechanisms underlying crocin biosynthesis in *C. x crocosmiiflora*, tran-scriptomic analysis was performed to identify key carotenoid cleavage dioxygenase (CCD) genes. Using *Crocus sativus* CsCCD2L gene as a bait, we identified a CCD transcript from the transcriptome data. Phylogenetic analysis revealed that the identified CCD belongs to the CCD2 subfamily, and it was designated as CroCCD2. Functional characterization of CroCCD2 was carried out using bacterial expression systems and *Nicotiana benthamiana* plants with a virus-mediated expression system. These experiments demonstrated that CroCCD2 efficiently converts the precursor zeaxanthin into crocetin, a key intermediate in crocin biosynthesis. Furthermore, we investigated the bioactivity of crocins and discovered that their anti-inflammatory effects depend on their vehiculation within exosomes or liposomes. This suggests that the transport mechanism is critical for the biological activity of crocins. Our findings highlight the specialization of CCD subfamilies in monocots and dicots for crocin biosynthesis and provide evidence of the anti-inflammatory activity of exosome-transported crocins. This study establishes a foundation for further research into the metabolic network of crocins in *C. x crocosmiiflora* and suggests that the CroCCD2 gene could be introduced into other crop plants to produce these bioactive apocarotenoids.

1. Introduction

Carotenoids are an important group of secondary metabolites that are widely distributed in nature, displaying key roles in all organisms [1]. In plants, carotenoids provide flowers and fruits with distinct bright colors ranging from yellow to red to attract pollinators and other animals that help in seed dispersal [2]. They also participate in photoprotection and photosynthesis [3], provide precursors for phytohormones [4–6], and possess a unique capacity for scavenging reactive oxygen species [7]. In humans, which are unable to synthesize

* Corresponding author.
E-mail address: marialourdes.gomez@uclm.es (L. Gómez-Gómez).
[1] These authors equally contribute to this work.

https://doi.org/10.1016/j.btre.2025.e00891
Received 24 January 2025; Received in revised form 12 March 2025; Accepted 27 March 2025
Available online 28 March 2025

carotenoids, these metabolites are relevant as precursors for vitamin A [8], and for their antioxidant activity that prevent cancer and other diseases including neurodegeneration or diabetes [9]. The carotenoid biosynthesis pathway in plants have been revealed by enzymatic and genetic studies [10], and genes underlying the central biosynthetic steps have been identified in many plants [11]. However, new enzymes are continuously discovered and characterized, which are involved in carotenoid cleavage [12] to produce apocarotenoids with different function [13]. The conjugated double bonds of the carotenoid structure can be target by the enzymes of a specific family, carotenoid cleavage dioxygenases (CCD), which catalyze the cleavage of the double bonds [14]. Thus, the abundance of targets in the wide number of different carotenoids present in nature, resulted in the generation of apocarotenoids with specific physic-chemical properties and particular biological functions.

Crocosmia × *crocosmiiflora* (Lemoine; Iridaceae), known as montbretia, is a monocotyledonous plant that was obtained from the cross of *C. aurea* and *C. pottsii*. The hybrid is broadly cultivated for their bright orange flowers. Different active metabolites have been isolated from flowers and corms of this hybrid [15–17]. The extracts obtained from the corms, characterized by the presence of saponins [18], have been used as antitumoral agents in Japanese traditional medicine [16]. The flowers contain crocins [19], which are reported to be active ingredients, responsible for various pharmacological actions including antioxidant and anti-inflammatory effects [20–22]. Crocins are glycosylated apocarotenoids, which accumulate in the flowers or fruits of few plant species [23,24], including species of the genus *Crocus* (Asparagales), with *C. sativus* as the principal producer among all *Crocus* species. Other plant species know to accumulate crocins are *Freesia* sps. (Asparagales), *Gardenia jasminoides* (Rubiales), *Buddleja davidii* (Lamiales), *Nyctanthes arbor-tristis* (Lamiales) and *Verbascum* sps. (Lamiales). The pathway for crocin biosynthesis has been elucidated in some of these species [23, 25–28]. The CCD that catalyzes the cleavage of the carotenoid substrate for the production of crocetin-dialdehyde is always localized in plastids, and are distributed in two subfamilies, based on recognition and cleavage of different substrates, including lycopene, β-carotene and zeaxanthin. In monocot species, such as those from *Crocus* and *Freesia*, the enzymes belong to the CCD2 subfamily, and recognize and cleavage zeaxanthin [25,28], while in dicots the enzymes belong to the CCD4 subfamily and show wider substrate specificity [29,30].

In this work, we have performed a comparative analysis of the crocin content in flowers of *Crocosmia x crocosmiiflora*. We have also identified the CCD2 enzyme involved in the crocin biosynthetic pathway in this hybrid species. Finally, we have isolated crocin-rich exosomes from the flowers and revealed a potential anti-inflammatory activity based on the effects on cell cultures.

2. Methods

2.1. Plant materials and sampling

Crocosmia x crocosmiiflora displays orange, tube shaped flowers distributed around a central axis (Fig. 1). Each branch can contain 4 to 20 flowers. The plants used in this study were grown in the Botanical Garden of Castilla-La Mancha (Albacete, Spain).

We collected flowers at preanthesis and anthesis, and further, flowers at anthesis were dissected in tepals, stamens and stigma. All materials sampled were immediately frozen in liquid nitrogen and then stored at −80 °C.

2.2. Pigment extraction

Polar (crocins) and nonpolar (crocetin and carotenoids) metabolites were extracted from 0.05 g of lyophilized flower tissues. For polar metabolites analyses, the tissues were extracted with 50:50 methanol:H_2O and sonicated for 10 min, followed by centrifugation and recover of the liquid phase. The insoluble fraction, was extracted with 2:1 $CHCl_3$: methanol to obtain the apolar metabolites. The obtained fractions were

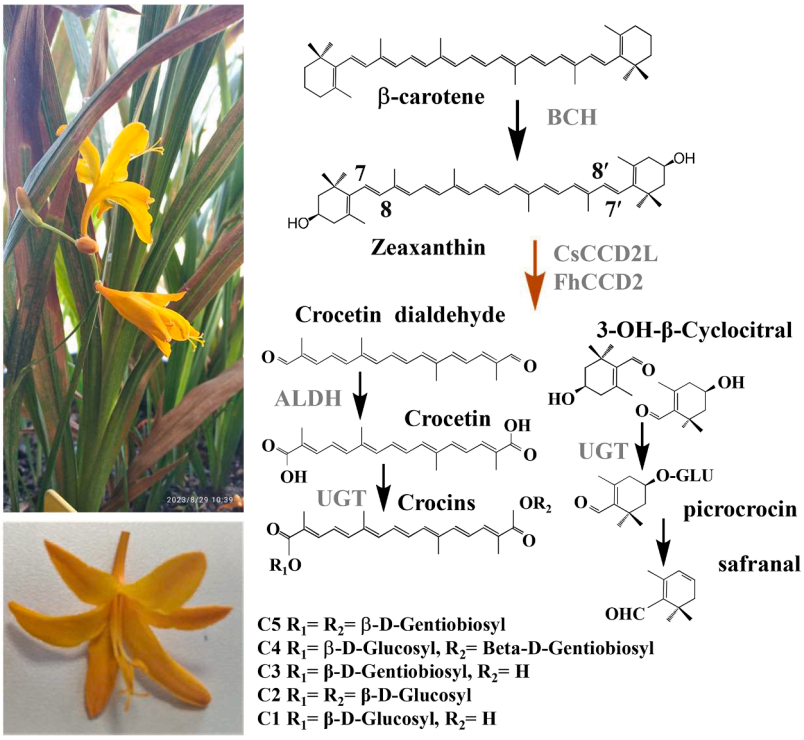

Fig. 1. *Crocosmia x crocosmiiflora* plants and flowers and a schematic overview of crocin biosynthesis pathway in *C. sativus* and *F. hybrida*. BCH, β-carotene hydroxylase; CsCCD2L, *C. sativus* carotenoid cleavage dioxygenase 2 L; PhCCD2, *F. hybrida* carotenoid cleavage dioxygenase 2; ALDH, aldehyde dehydrogenase; UGT, UDP-glucosyltransferases.

analyzed separately by chromatographic methods as described below.

2.3. Carotenoid cleavage dioxygenase identification, isolation, and cloning

CCD2 amino acid sequences from *C. sativus* and *C. ancyrensis* were applied as queries to search candidate CCDs in the *Crocosmia x crocosmiiflora* Bioproject PRJNA389589 using BLASTN (https://blast.ncbi.nlm.nih.gov/). The obtained sequence was used for the design of specific oligonucleotides: 5′-CATGGATGCATCTAAACCTCTGCTGT-3′ and 5′-TCATGCCTCTGCTTGCTGCTTCTGAAGT-3′, for the isolation and cloning of the corresponding cDNA, using total RNA extracted from flowers with the TRIzol™ reagent (Invitrogen) according to the manufacturer's instructions, and treated with RNase-free DNase I (Promega) to remove any residual genomic DNA. Oligo dT was used to synthesize first-strand cDNA with the Ready-To-Go You-Prime First-Strand Beads (Cytiva). The obtained cDNA was used as template for a PCR reaction using the following conditions: 95 °C for 5 min; 40 cycles of 94 °C for 5 s, 55 °C for 20 s, and 72 °C for 2 min. The PCR products were loaded in a 1 % agarose gel, and the selected product purified, cloned in the pGEM®-T Easy Vector (Promega) and sequenced. Further, the oligonucleotides: 5′-CGCCCTTGGCGAATTCATGTTCCTTCCACGTAAACGGTGC-3′ and 5′-TACCCTCGAGGAATTCACTCTTCCGATCTCTCTGCTTGCTG-3′ were used to clone the cDNA into the pThio-Dan vector (Invitrogen). The resulting expression plasmid, designated as pThio-CroCCD2, was assembled using the In-Fusion® HD Cloning Plus CE kit (Takara) and sequenced to verify accurate assembly and the absence of sequence errors.

2.4. Phylogenetic relationship

Multiple sequence alignment with CCD amino acid sequences was carried out using MEGA 11.0.10 program (https://megasoftware.net/) to construct the phylogenetic tree of the aligned sequences using the Maximum Parsimony method with 2500 bootstrap replicates.

2.5. Expression in carotenoid-accumulating E. coli cells

Carotenoid-accumulating *Escherichia coli* BL21 cells harboring different PAC-plasmids (chloramphenicol resistance) to produce carotenoids, were transformed either with pThio-CroCCD2 (ampicillin resistance) or the void pThio-vector (ampicillin resistance) which was used as negative control. Clones were selected by their corresponding antibiotic resistance and overnight cultures were grown at 30 °C in 5 mL of 2YT-medium and were used to inoculate 50 mL of 2YT-medium. Expression of CroCCD2 was induced with 0.2 % (w/v) arabinose when an optic density at 600 nm (OD600) of 0.5 was reached and further incubated at 30 °C for 4–6 h, followed by centrifugation. The pellets were resuspended in 2 mL of acetone, and 2 mL of diethyl ether: petroleum ether (1:2), mixed by vortex and sonicated for 10 min. After, 2 mL H_2O were added, mixed by vortex and centrifuged for 5 min at 10,000 x g. The organic pigmented phase containing lipophilic compounds was dried and the residue redissolved in 400 µL ethyl methyl butyl ether for chromatographic analyses.

2.6. HPLC analysis

The soluble fraction, containing crocins, was analyzed by HPLC-DAD-HRMS (Thermo Fisher Scientific) [31]. The apolar fraction containing carotenoids and *E. coli* pigments fractions were analyzed on a reverse-phase HPLC system equipped with a photodiode array detector (Agilent Technologies). The compounds were separated at a flow rate of 1 mL min^{-1} using a C30 column (150 × 3 mm i.d., 5 µm) (YMC Europa, Schermbeck, Germany) and the following solvent system: A: methanol/H_2O (98:2, v/v), B: methanol/H_2O (95:2, v/v) and C: TBME. The elution gradient began at 80 % A and 20 % C at 0 min, then moving linearly to 60 % A and 40 % C by 3 min. At 4 min, the gradient shifted to 60 % B and 40 % C, then transitioned linearly to 0 % B and 100 % C by 12 min, before returning to the initial conditions by 13 min. Metabolite identification relied on absorption spectra and retention times relative to standard compounds.

2.7. Activity assays in N. benthamiana

Plasmid pGTEV-CroCCD2 was constructed by PCR amplification of the cDNA of CroCCD2 (Supplementary Table S1) and Gibson DNA assembly (New England Biolabs); plasmid pGTEV-CsCCD2L was obtained as previously described, including NIb in the viral clone [30]. The plasmid to express a green fluorescent protein (pGTEV-aGFP) was previously described [30]. Competent *A. tumefaciens* strain C58C1 containing the helper plasmid pCLEAN-S48, were independently transformed by electroporation with the plasmids pGTEV-CroCCD2, pGTEV-CsCCD2L, and pGTEV-aGFP, and selected in plates containing 50 µg/mL kanamycin, 50 µg/mL rifampicin, and 7.5 µg/mL tetracycline. Liquid cultures of selected positive colonies were used to infiltrate one leaf of one-month-old *N. benthamiana*. After infiltration, plants were transferred to a plant growth chamber with 16–8 h day-night photoperiod at 25 °C. Leaf tissue was collected 14 days post-inoculation (dpi) and analyzed for crocin and carotenoid content.

2.8. Exosome isolation and characterization

Nanovesicles were purified from *Crocosmia x crocosmiiflora* flowers by modifying a method previously used to isolate plant exosomes by sequential centrifugations [32,33]. The flowers were weighed, and the same amount of 1 x phosphate-buffered saline (PBS) added. The mixture was kept stirring for 20 min and subjected to low-speed centrifugation (2000 × g 20 min and 5000 × g 40 min) to remove large particles and fibers. Intact organelles were removed by centrifugation at 10,000 × g for 60 min. The obtained supernatant was ultra-high-speed centrifugated (180,000 × g, 60 min) to pellet the exosome-like nanovesicles. The obtained pellet was washed once with 1 x PBS and resuspended in 1 x PBS. To determine the total protein content of exosome-like nanovesicles, a MicroBCA Protein Assay Kit (Thermo Fisher Scientific) was used, following manufacturer's instructions. The exosomes were aliquoted and stored at −80 °C until used.

2.9. Preparation of liposomes with crocosmia x crocosmiiflora polar extract

Liposomes were prepared using thin-film hydration followed by the extrusion method previously described [34]. In brief, 90 mg of phosphatidylcholine and 10 mg of cholesterol were dissolved in 4 mL $CHCl_3$ in a round-bottomed flask and the solvent was evaporated on a rotary vacuum evaporator at 40 °C until a lipid thin film was obtained. The film was hydrated with 10 mL of previously prepared *Crocosmia x crocosmiiflora* polar extract (in 1 x PBS), rotating the flask at 40 °C without vacuum. Finally, the vesicles were extruded with the Avanti Polar Lipids Mini Extruder set through 0.1 µm polycarbonate membranes performing a total of 30 passes. Samples were stored at 4 °C until use.

2.10. Liposomes and extracellular vesicles characterization by transmission electron microscopy (TEM)

The exosomes and liposomes isolated form *Crocosmia x crocosmiiflora* were characterized by TEM at the Centro de Investigación Principe Felipe (CIPF; Valencia, Spain) electron microscopy facility as previously described [35]. Briefly, 20 µL of nanovesicles suspension were loaded onto formvar carbon-coated grids, negatively stained with an aqueous phosphotungstic acid solution for 60 s and imaged using a FEI Tecnai G2 Spirit Biotwin 120 kw microscope.

2.11. Cell culture model

Raw 264.7 cells (ATCC No TIB-71) at 1.50 × 10^5 cells/cm^2 were grown in Dulbecco's modified Eagle's medium (DMEM) (Lonza) that was supplemented with 2 mM l-glutamine, 100 U/mL penicillin-streptomycin, 10 % FBS, and, incubated at 37 °C in a 5 % CO_2 incubator. The cells were treated with 25 μg/mL protein from *Crocosmia x crocosmiiflora* exosomes (Exos-Crocos), crocosmia polar extract (Ext-Crocos), liposomes (Lipo), and liposomes with encapsulated *Crocosmia x crocosmiiflora* extract (Lipo-Crocos). Dexamethasone (DEX), a potent glucocorticoid possessing anti-inflammatory properties, which inhibits the expression of inflammatory mediators by macrophages and other cells and is used in the treatment of many immune-mediated inflammatory diseases [36] was used as a positive control at 1 μM, and cultured overnight in DMEM containing 5 % FBS, before activation using 150 ng/mL LPS from the bacteria *Salmonella typhimurium* (Sigma-Aldrich).

2.12. Nitric oxide (NO) determination

Nitrite, an indicator of the production of NO, was evaluated using the Griess reagent system (Promega). Briefly, RAW264.7 cells were cultivated in 10 % FBS-DMEM and treated as stated before. Nitrite levels were measured in the supernatants using the Greiss reagent. Absorbance values at 560 nm were recorded and compared with a nitrite standard curve using a spectrophotometer.

2.13. RNA isolation and reverse transcription quantitative polymerase chain reaction (qPCR) of treated Raw 264.7 cells

The TRIzol reagent (Invitrogen) was used for total RNA extraction from cells, and RNA concentrations determined in a ND-1000 (NanoDrop) spectrophotometer. cDNA synthesis was performed using 1 μg of total RNA using the RevertAid H Minus First Strand cDNA Synthesis kit (Thermo Fisher Scientific). SYBR® Premix (Applied Biosystems™) was used for the qPCR reactions, performed in a Light Cycler 96 Real-Time PCR System (Applied Biosystems™). The mouse riboprotein P0 housekeeping gene was used for normalization. The primers used for the expression analyses are shown in Table S1.

2.14. Protein extraction and western blotting

RAW264.7 cells were collected by washing twice with 1 x PBS, detaching them from the culture dishes, followed by centrifugation. The cells were subsequently resuspended in RIPA lysis buffer (0.2 mM EDTA, 1 % Triton X-100, 1.5 mM $MgCl_2$, 0.3 M NaCl, 0.1 % SDS, 20 mM β-glycerophosphate, 0.5 % deoxycholic acid, and 25 mM HEPES at pH 7.5), followed by the addition of protease and phosphatase inhibitors (Sigma). The mixture was homogenized on a shaker for 30 min at 4 °C and then centrifuged at 10,000 × *g* for 15 min. Protein concentration was determined using the Pierce™ BCA Protein Assay Kit (Thermo Fisher Scientific). Protein extracts (40 μg) were resolved on a 10 % SDS-PAGE gel and transferred to PVDF membranes (Hybond™, Amersham GE Healthcare Life Sciences). The membrane was blocked for 1 h at room temperature following the manufacturer's protocol and then incubated overnight at 4 °C with the primary antibody followed by incubation with secondary antibodies at 37 °C for 1 h. The antibodies included anti-Mouse INOS (#610,432) and Anti-Mouse COX2 (#610,204) from BD Biosciences, while Anti-ERK2 (sc-154) was sourced from Santa Cruz Biotechnology. Detection of immunoconjugates was performed using an enhanced chemiluminescence (ECL) substrate (Santa Cruz Biotechnology) with a chemiluminescence imaging system (Bio-Rad). ERK2 expression served as a loading control for the extracts and was used for calculation of relative protein levels using ImageJ software.

2.15. Enzyme linked immunosorbent assay (ELISA)

RAW264.7 cells were plated in 6-well plates at a density of 3 × 10^6 cells per well and subsequently exposed to Exos-Crocos, Ext-Crocos, Lipo, and Lipo-Crocos (25 μg/mL), or DEX (1 μM). The cells were maintained overnight in DMEM supplemented with 5 % FBS. Following this incubation, they were stimulated with LPS (150 ng/mL) for 8 h. Post-treatment, the culture supernatants were harvested, and the concentrations of IL-1β, IL-6, and TNF-α were quantified using ELISA kits, following the manufacturer's instructions (Ready-Set-Go kit, eBioscience).

2.16. Statistical analysis

The obtained results were expressed as the mean ± standard deviation (SD) based on a minimum of three independent experiments or with the number of replicas indicated in the text. Statistical analysis is specified in the figure legends, when applicable.

3. Results

3.1. The content of crocins differs among the flower organs in Crocosmia x crocosmiiflora

The flowers of *Crocosmia x crocosmiiflora* exhibit bright orange tepals, stigmas and stamens (Fig. 1). Polar extracts were obtained from flowers at anthesis, and a total of 18 peaks were identified in the chromatograms with maximum absorbances between 435 and 468 nm (Fig. S1A). Further, the flowers were dissected, and tepals, stigma and stamens were analyzed separately by HPLC-DAD-HRMS (Fig. 2A and B). Mass spectrometry chromatograms from the detected peaks at 440 nm revealed the presence of the crocetin aglycon (*m/z* 329.1747 (M + H)) (Fig. 2B). Analyses of the sugar moieties associated with the crocetin molecule led to the identification of crocins with varying glucosylation patterns from 1 to 8 glucose molecules. Tepals were the tissue with higher content of crocins detected, 83.7 %; followed by the stigma, 11.6 % and the stamens, 4.7 % (Fig. 2C). The predominant crocins were those conjugated with 8 glucose molecules, followed by those with 6 and 7 units.

Carotenoid extracts without saponification were also analyzed by HPLC-DAD in flowers at anthesis. The carotenoids neoxanthin, zeaxanthin, α-carotene and β-carotene were identified as the main carotenoids present in tepals (Fig. S1C).

3.2. Identification of a CCD2 enzyme involved in the biosynthesis of crocetin dialdehyde

Raw transcriptome reads from the Bioproject PRJNA389589 were searched using the sequence of CsCCD2L from saffron, and the homolog from *C. ancyrensis* [26]. A unique sequence of 1839 nt was found, which showed 87.58 % identity with CsCCD2L (KP887110) at the nucleotide level, and 87.96 % and 88.07 % identity with the CCD2 nucleotide sequences from *C. ancyrensis* (KP792756.1) and *C. Chrysanthus* (KP887108.1), respectively. The pulled sequence encoded a protein of 597 amino acids, with a theoretical molecular weight of 66.83 kDa, and an isoelectric point of 6.43. This protein was named CroCCD2. This amino acid sequence was used to construct a phylogenetic tree with those of other CCDs known to catalyze the biosynthesis of crocins in other plants (Fig. 3). The sequences grouped in two clearly separated clusters containing the monocot and the dicot sequences, respectively. The CroCCD2 was closely related to the CCD2 from *Freesia x hybrida* (Fig. 3).

A cDNA corresponding to CroCCD2 was isolated using RNA purified from flower tissue. This cDNA was cloned in the expression vector pTHIO-Dan1 to test the cleavage activity using *E. coli* cells producing and accumulating different carotenoid substrates [37]. Hence, we

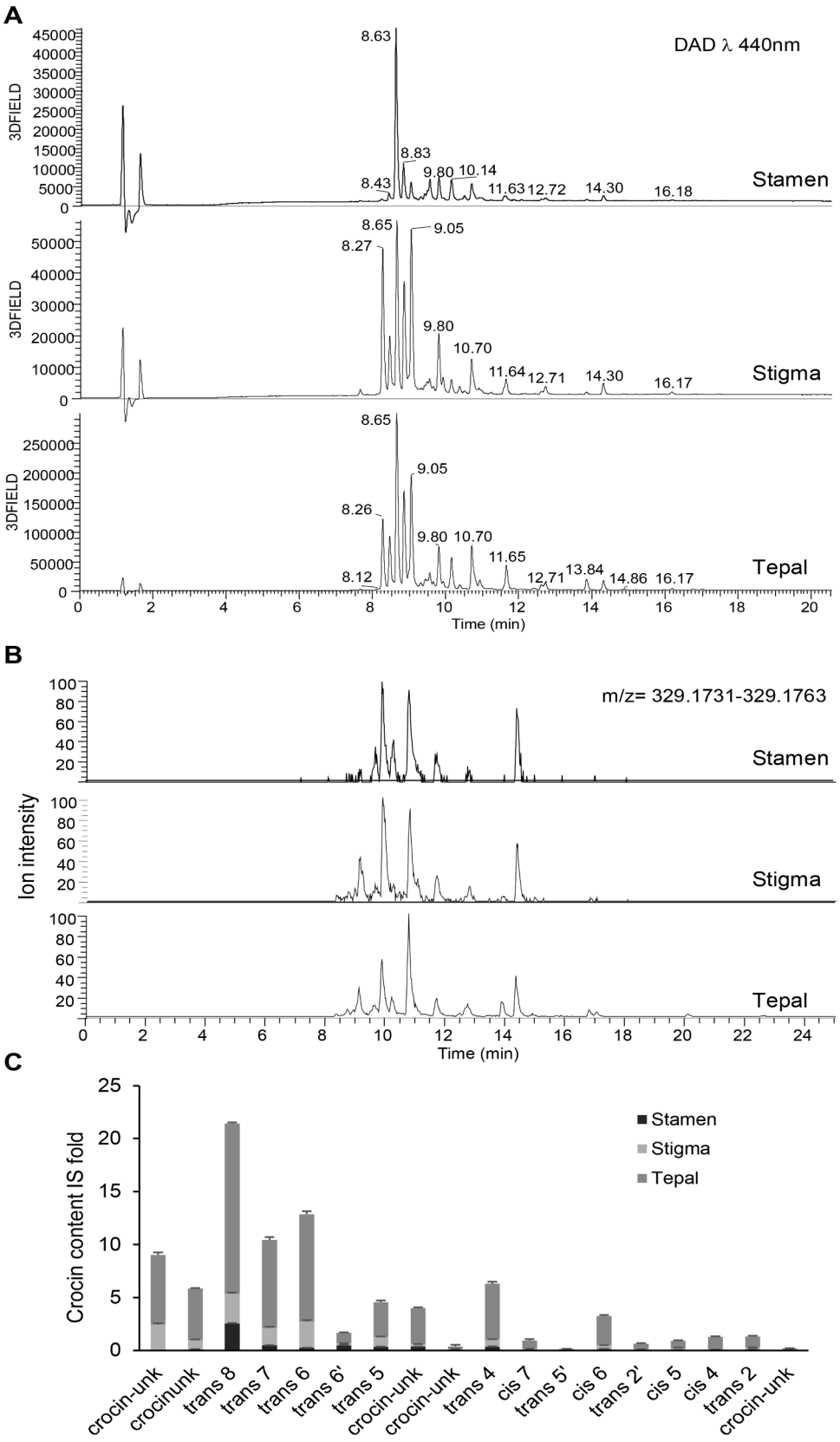

Fig. 2. Crocin analysis of polar extracts obtained from different tissues of Crocosmia x crocosmiiflora flowers. (A) PDA chromatograms obtained by HPLC-DAD-HRMS at 440 nm. (B) HPLC-ESI(+)-HRMS system, extracting crocetin aglycon mass (m/z = 329.1731–329.1763) from the polar extracts from stamens, stigmas and tepals. (C) Levels of crocins and crocetin in stamens, stigmas and tepals. Data are the average ±SD of at least three independent biological replicates and are expressed as fold internal standard (IS) values.

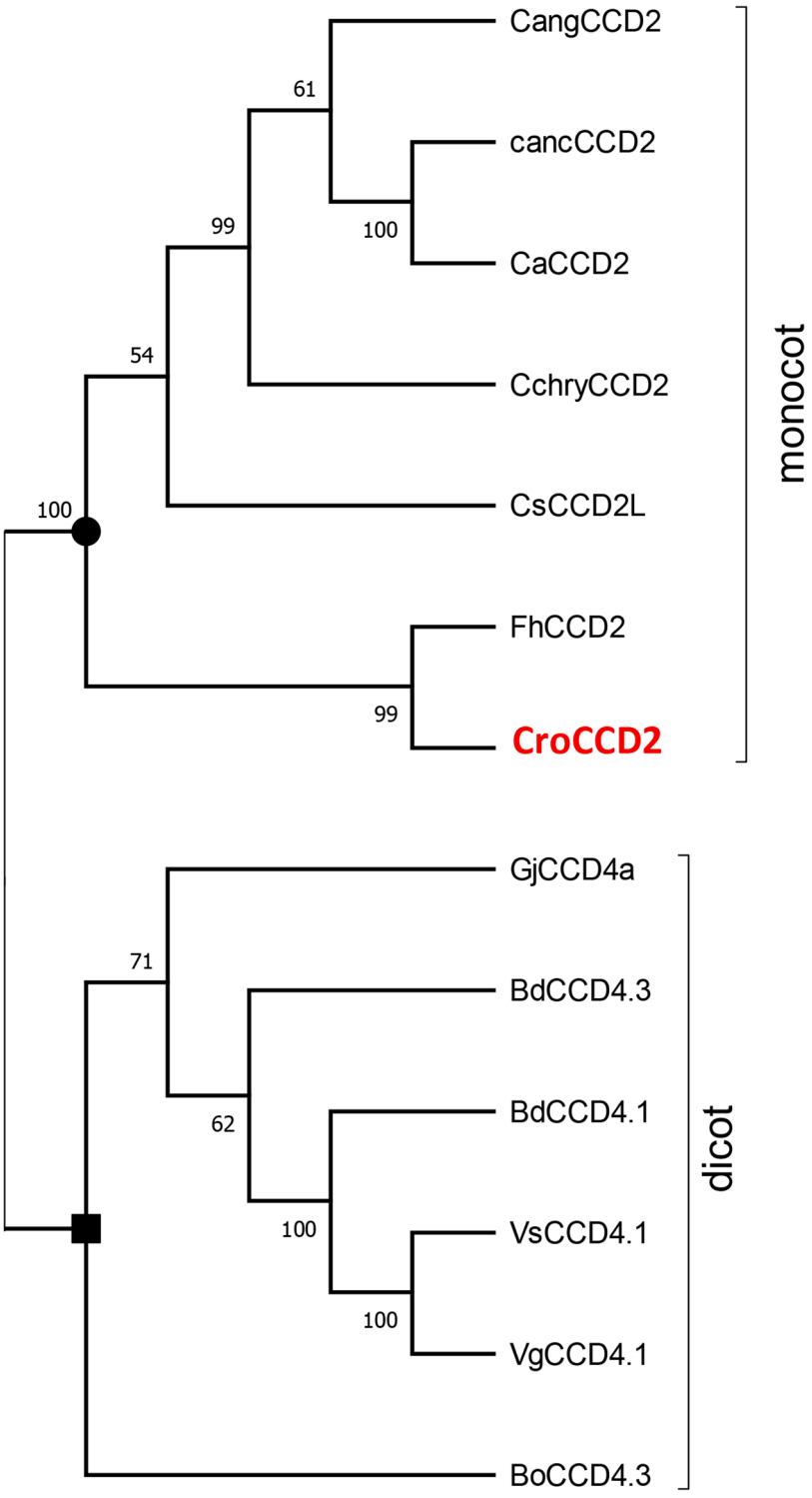

Fig. 3. Maximum parsimony analysis of 13 selected amino acid sequences of CCD enzymes catalyzing the biosynthesis of crocins in plants known to accumulate these apocarotenoids. The evolutionary history was inferred using the maximum parsimony method. The bootstrap consensus tree inferred from 2000 replicates is taken to represent the evolutionary history of the taxa analyzed. Branches corresponding to partitions reproduced in <50 % bootstrap replicates are collapsed. The percentage of replicate trees in which the associated taxa clustered together in the bootstrap test (2000 replicates) are shown next to the branches. The MP tree was obtained using the Subtree-Pruning-Regrafting (SPR) algorithm with search level 1 in which the initial trees were obtained by the random addition of sequences (10 replicates). Evolutionary analyses were conducted in MEGA11 (https://www.megasoftware.net/). CroCCD2 is highlighted in red.

expressed CroCCD2 in lycopene, β-carotene and zeaxanthin accumulating *E. coli* and analyzed the cleavage activity and substrate specificity by HPLC and HPLC-DAD-HRMS. In the zeaxanthin background, CroCCD2 produced a compound that was identified as crocetin dialdehyde (Fig. 4A). However, in β-carotene and lycopene-accumulating bacteria, we did not detect any product. These data indicate that CroCCD2 only recognized zeaxanthin and cleaves the C7′-C8′ and the C7-C8 double bonds to produce crocetin dialdehyde.

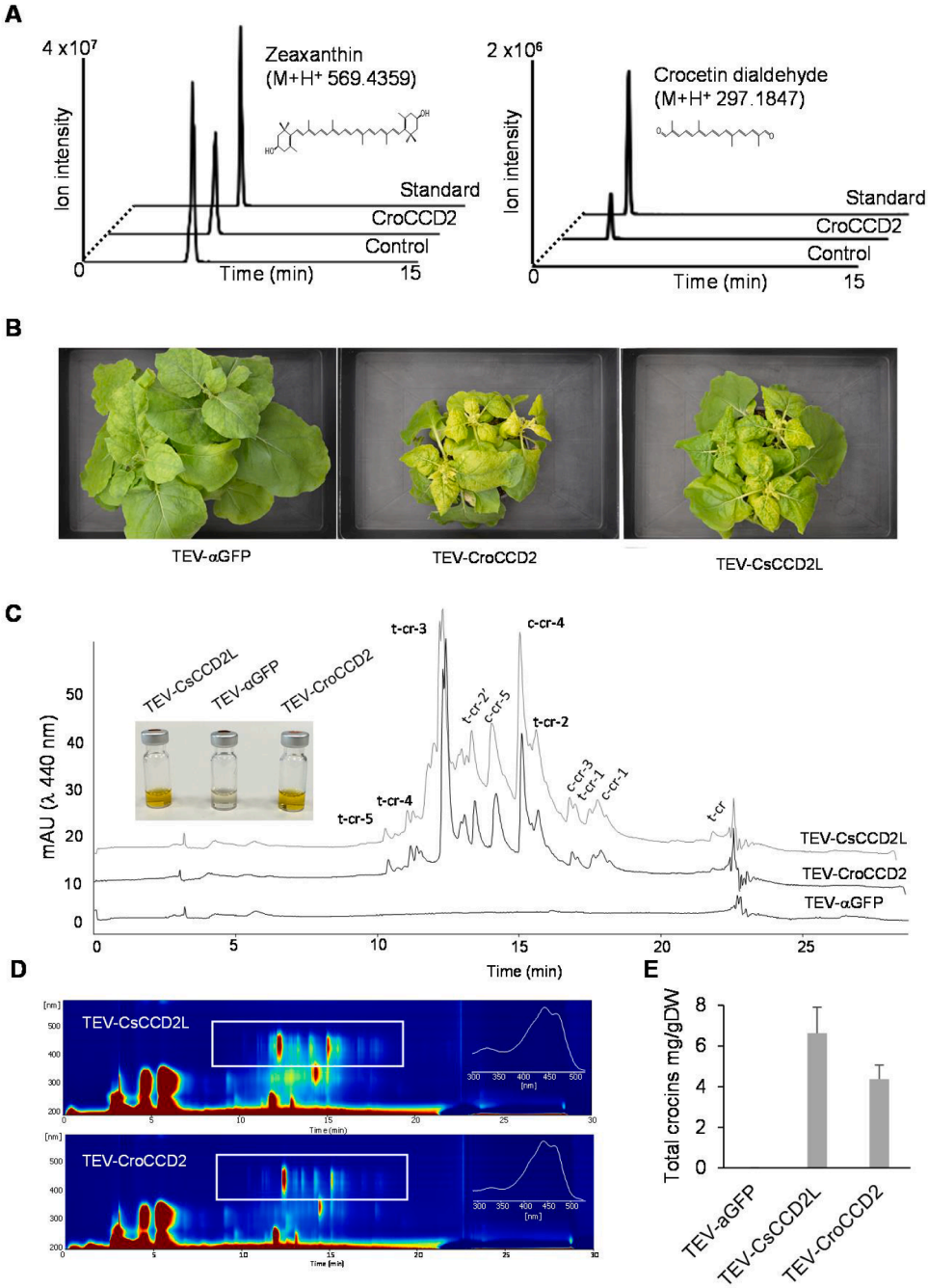

Fig. 4. Activity assays of CroCCD2 in *E. coli* and *N. benthamiana* plants. (A) Chromatograms obtained by HPLC—HRMS of the *in vivo* assays of CroCCD2 expressed in *E. coli* accumulating zeaxanthin. Induction of CroCCD2 in these cells converted zeaxanthin into crocetin dialdehyde. (B) Pictures of representative leaves from plants agroinoculated with TEV-αGFP, TEV-CroCCD2 and TEV-CsCCD2L, as indicated, taken at 14 dpi. Scale bars correspond to 5 mm. (C) Chromatographic profile run on an HPLC-PDA and detected at 440 nm of the polar fraction of *N. benthamiana* leaves infected with TEV-aGFP, TEV-CsCCD2L, and TEV-CroCCD2. Peaks abbreviations correspond to: c-cr, cis-crocetin; t-cr, trans-crocetin; c-cr1, cis-crocin 1; t-cr1, trans-crocin 1; t-cr2, trans-crocin 2; t-cr2', trans-crocin 2'; c-cr3, cis-crocin 3, t-cr3, trans-crocin 3; c-cr4, cis-crocin 4; t-cr4, trans-crocin 4; c-cr5, cis-crocin 5; t-cr5, trans-crocetin 5. (D) HPLC-DAD/UV isoplot chromatograms of polar extracts from TEV-CsCCD2L, and TEV-CroCCD2, and inset is shown the absorbance spectra of trans-crocin 3, the major crocin detected in the polar extracts. (E) Quantification of crocins in the polar extracts obtained from *N. benthamiana* leaves infected with TEV-αGFP, TEV-CsCCD2L, and TEV-CroCCD2, was performed by HPLC analysis. Data are represented as mean ± SD of three independent pools of infected *N. benthamiana* plants.

3.3. Analysis of N. benthamina leaves infected with an engineered viral vector designed to express CroCCD2

Using the tobacco etch virus (TEV)-based system previously developed to express CsCCD2L [31], we investigated the production of crocins in *N. benthamiana* through the expression of CroCCD2. We introduced the cDNA of CroCCD2 into the amino terminus of the viral polyprotein. The obtained recombinant clone TEV-CroCCD2 was agroinoculated in *N. benthamiana* plants. As a negative and positive controls, plants were agroinoculated with TEV-aGFP and TEV-CsCCD2L, respectively [30]. The plants inoculated with TEV-CroCCD2, TEV-CsCCD2L, and TEV-aGFP showed the first symptoms of infection at approximately 8 dpi. At 14 dpi, the leaves of plants infected with TEV-CroCCD2 and TEV-CsCCD2L exhibited spots and areas with a yellow coloration,

indicative of crocin accumulation (Fig. 4B). Chromatographic analysis of polar extracts revealed peaks at different retentions times corresponding to crocins in TEV-CroCCD2 and TEV-CsCCD2L (Fig. 4B). These peaks were absent in the corresponding polar extracts from tissues of mock-inoculated plants or control plants agroinoculated with TEV-aGFP (Fig. 4C). Crocin quantification resulted in 4.37 ± 0.07 mg and 6.63 ± 1.28 mg of crocins per gram of *N. benthamiana* dry weight (DW) leaf tissue in TEV-CroCCD2 and TEV-CsCCD2L, respectively. Thin layer chromatography (TLC) and HPLC-DAD analyses of apolar extracts containing carotenoids and chlorophylls revealed a reduction in both types of metabolites in samples infected with all viral vectors, particularly those infected with TEV-CroCCD2 and TEV-CsCCD2L (Fig 4S). The most evident differences were observed at the level of chlorophylls and xanthophylls. Overall, the obtained results revealed a notable accumulation of crocins in plants expressing CroCCD2 and CsCCD2L.

3.4. *Anti-inflammatory effect of crocins extracts in LPS-challenged RAW 264.7 cells*

Several approaches were followed to determine the potential anti-inflammatory activity of the crocins from *Crocosmia x crocosmiiflora* (Fig. 5A). In our first attempt, we evaluated lipopolysaccharide (LPS)-induced nitric oxide (NO) production in RAW 264.7 cells, which were pre-treated directly with the crocin extract (125 μg/mL) obtained from *Crocosmia x crocosmiiflora* flowers. We observed that LPS-induced NO release was not suppressed compared with non-treated cells (Fig. 5C),

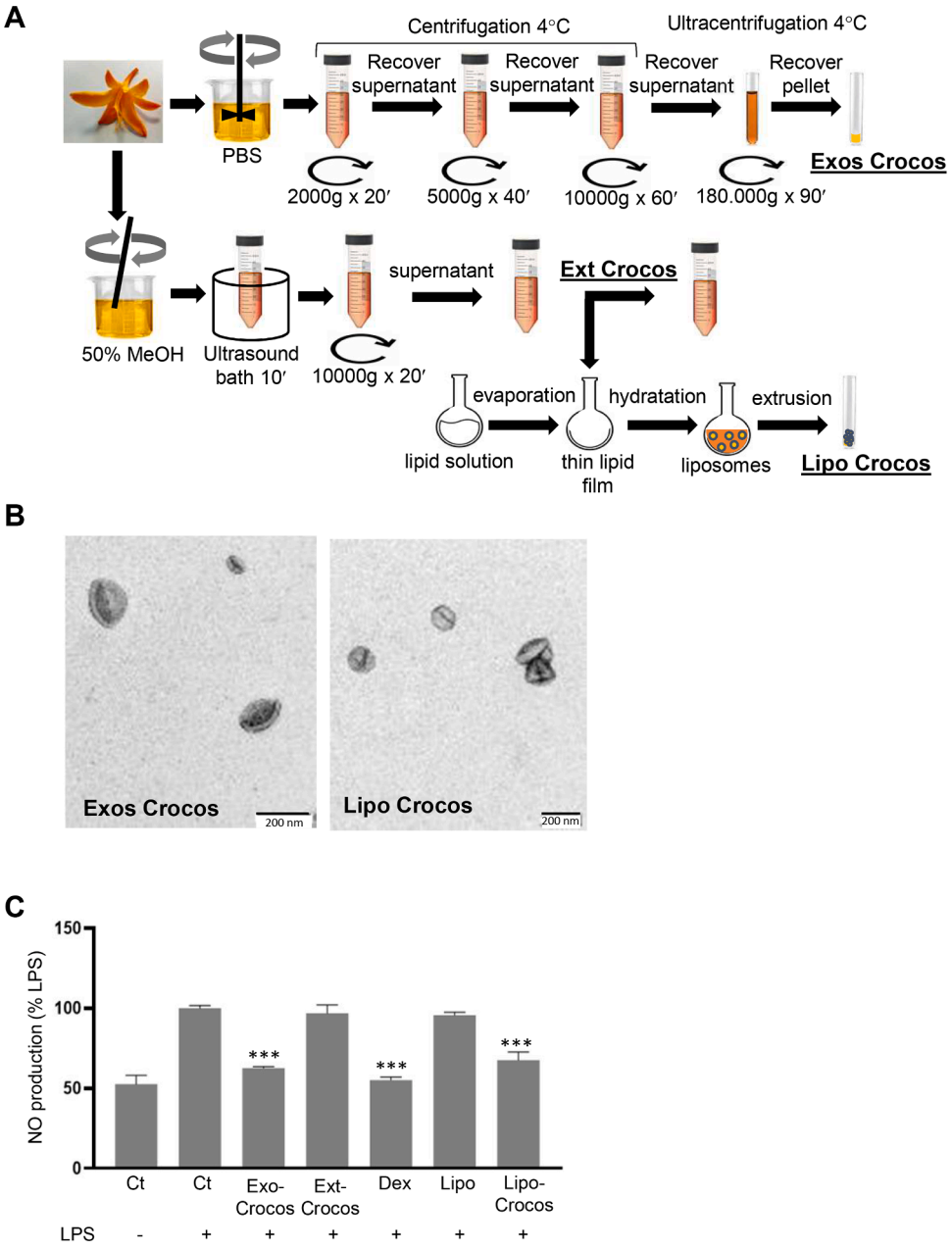

Fig. 5. Samples tested for anti-inflammatory activity on LPS-activated RAW264.7 cells. (A) Schematic presentation of the procedures followed for the obtention of the three samples tested: exosomes of *Crocosmia x crocosmiiflora* (Exos Crocos), crocins extracts obtained by 50 % methanol extraction of *Crocosmia x crocosmiiflora* flowers (Ext Crocos), and the encapsulated crocins in liposomes (Lipo Crocos). (B) Transmission electron microscopy imagen of nanovesicles isolated from *Crocosmia x crocosmiiflora* (Exos Crocos). Scale bar is 100 nm. (C) Effects of Exos Crocos, and Lipo Crocos on nitric oxide production in LPS-stimulated RAW 264.7 cells. The amount of nitric oxide produced was then determined using Griess assay. Data are expressed as mean ± SD. n = 3. *p < 0.05 and **p < 0.01 vs. using One-way ANOVA and Dunnett's post-hoc test.

suggesting that the penetration of such hydrophilic components into the cells was mostly impeded by the water impermeable barrier of the membrane. To test this possibility, we follow two different strategies. First, we decided to isolate exosomes from *Crocosmia x crocosmiiflora* flowers (Fig. 5A). Starting from collected fresh flowers, we obtained preparations of Exos-Crocos with a final protein concentration of 18.80 μg/μL. Our procedure enabled the recovery of visible pellets, which were further purified through multiple washing steps. This resulted in a uniform and purified exosome preparation, displaying a round-shaped vesicular morphology with a characteristic lipid bilayer, as observed using transmission electron microscopy (TEM) images (Fig. 5B). The second strategy consisted in the use of liposomes, as the artificial counterparts to exosomes. Liposomes were successfully prepared using the thin layer hydration method (Fig. 5A). The encapsulation efficiency of the obtained liposomes was 68 %. This was calculated based on the ratio between the concentrations of the incorporated crocin in the formulation over the initial concentration in the extract (Fig. S5). The particle size of the Lipo-Crocos was in the range of 50–150 nm, as determined by TEM analysis (Fig. 5B). Exos-Crocos and Lipo-Crocos, both suppressed NO production prior to LPS stimulation in comparison to non-treated cells (Fig. 5C). Further, we evaluated the expression of the inducible nitric oxide synthase (INOS), which produces NO from l-arginine. INOS mRNA expression levels induced by the LPS treatment were reduced in the cells treated with dexamethasone, Exos-Crocos, and Lipo-Crocos (Fig. 6A), similar results were obtained as well at the protein levels (Fig. 6B).

To determine the anti-inflammatory mechanism of Exos-Crocos, and Lipo-Crocos, the mRNA levels of the major pro-inflammatory enzyme COX2, and pro-inflammatory IL-1b, IL-6, IL-10, TNF-α and IFN-β cytokines were analyzed by real time quantitative PCR (Fig. 6A). Results show that the treatment of cells with LPS induced the expression of all the tested genes compared to control (Fig. 6A), and the induction was also observed for the cells treated with LPS and Ext-Crocos (Fig. 6A). However, cells treated with LPS and Exos-Crocos, or Lipo-Crocos concentration decreased the LPS induced mRNA level of all the genes tested (Fig. 6A). Major reduction of the transcript levels was observed for TNF-α and COX2 (Fig. 6A), while the reduction of expression was more

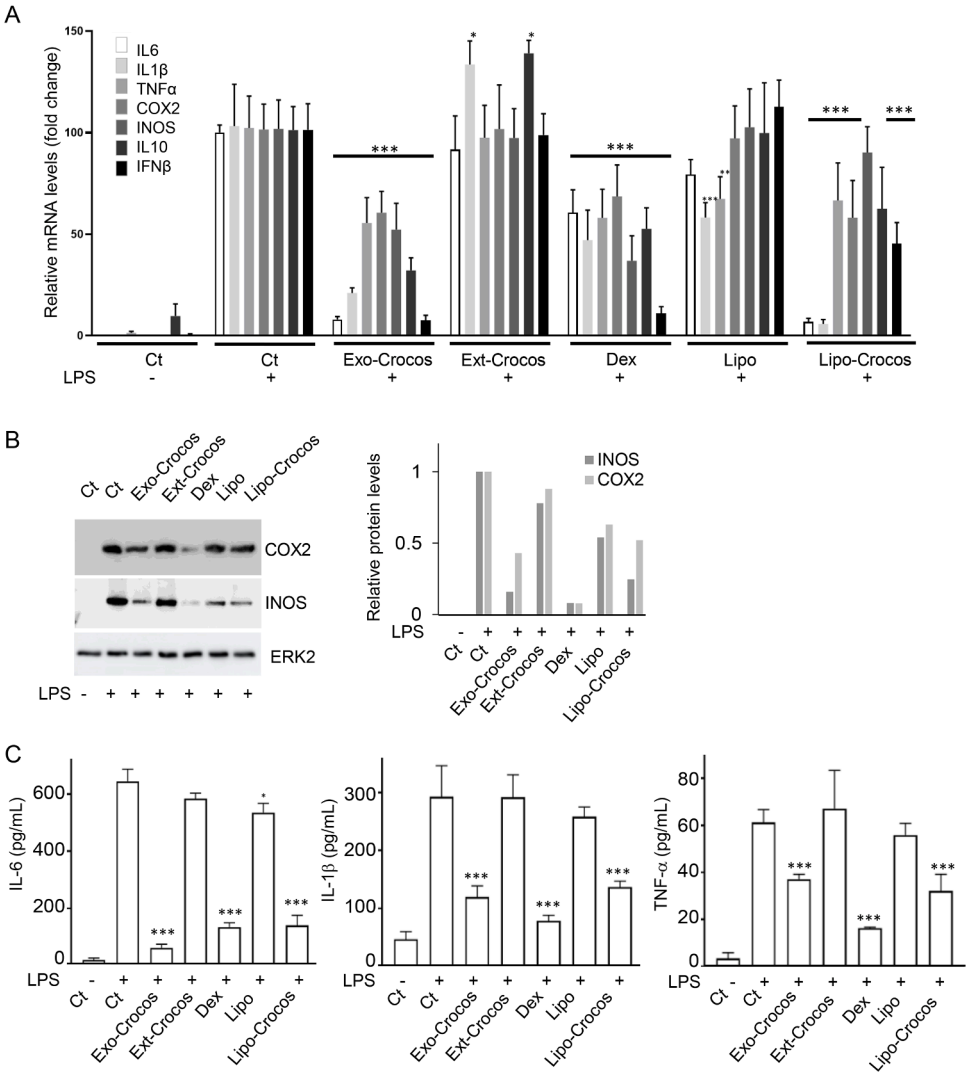

Fig. 6. Anti-inflammatory effect of Exos Crocos, and Lipo Crocos in RAW264.7 cells. (A) Changes on the relative mRNA expression levels of iNOS, IL-6, IL-1β, TNF-α, COX2, INFb, and IL-10 mRNA levels in LPS-stimulated RAW264.7 cells treated with and without Exos Crocos, and Lipo Crocos and compared with the effects of Dex in LPS-stimulated cells. (B) LPS-induced changes and the effect of the different treatments in the protein levels of COX-2 and INOX were determined by Western blot analysis. ERK2 was used as a loading control. Data were expressed as a ratio relative to the LPS alone group. (C) Secretion of IL-1β, IL-6 and TNFα in the supernatants of the cell cultures under the different tested conditions were detected by ELISA. Protein marker: M; Control: Ct; Exosomes: Exo; Extract: Ext; Dexamethasone: Dex; Liposomes: Lipo; Liposomes with extract: Lip Ext. Data are expressed as mean ± SD. n = 3. *p < 0.05 and **p < 0.01 vs. using One-way ANOVA and Dunnett's post-hoc test.

evident for IL-1β, IL-6, IL-10, and IFN-β (Fig. 6A). Similar results were obtained when the protein levels of COX-2, IL-1β, IL-6, and TNF-α were evaluated (Fig. 6B and C). COX2 protein levels were increased after the treatment with LPS (Fig. 6B), while in cells treated with LPS and Exos-Crocos, Lipo-Crocos or DEX the protein levels were reduced (Fig. 6B). The evaluation of IL-1β, IL-6, and TNF-α secretion in the supernatant of RAW264.7 cells treated with LPS showed a significant elevation in the production of these cytokines compared with the control group non treated with LPS (Fig. 6C), and this reduction was observed in the supernatant of cells treated with LPS and Exos-Crocos, Lipo-Crocos or DEX (Fig. 6C).

4. Discussion

Actual lifestyles continuously expose individuals to a wide array of stimuli coming from multiples and diverse sources. This continued exposition may act as a potential trigger for long-term oxidative stress, inflammation, and the onset of chronic diseases [38]. Crocins are well known to combat ROS production and these apocarotenoids suppress the secretion of pro-inflammatory cytokines but also reduce inflammation in various organs/systems, as demonstrated in a series of animal models and *in vitro* experiments [21,39,40]. Significant research has been conducted during the last decade on the health effects of crocins in pharmacological studies, leading to an increasing demand for these apocarotenoids within the pharmaceutical industry [41]. However, crocins biosynthesis is limited to a few plant species, and inside these species, crocins accumulation is temporal and tissue-regulated, found mainly in flowers and fruits [23,30,42,43], which hampers the uninterrupted availability of these compounds for a large spectrum of pharmaceutical and food applications [44]. Therefore, the identification of new plant species accumulating crocins is desired.

4.1. Highly glycosylated crocins are the major crocins in flower tissues

In this study, we have investigated the presence and accumulation of crocins in the monocotyledonous plant *Crocosmia x crocosmiiflora*. The orange flowers accumulate crocins with a high number of glucose molecules in all the tissues, including stamens, stigma and tepals. Crocin with 8 glucose molecules was identified as the major component, followed by crocins with six and seven glucose molecules. The predominant occurrence of these extensively glycosylated crocins had not been previously detected in any plant recognized for accumulating crocins, despite their prior identification in spring crocuses [45]. The total concentration of crocins in dry tepals reach 87.32 ± 3.3 mg/g DW. This value is comparable to the value reported for the crocins content in the corolla tubes of *B. davidii*, ranging from 71.6 to 56.6 mg/g, and above the quantities present in the dry fruits of gardenia (from 10.08 to 36.97 mg/g DW) and *Verbascum* species (from 14.38 to 9.87 mg/g DW), but still below the concentration from crocins in the stigma of saffron (from 170 to 317 mg/g DW) [30]. Nevertheless, as transcriptional regulation is considered the primary mechanism controlling crocins biosynthesis, crocin content varies depending on the developmental stage of the tissue, environmental conditions, and species-specific factors, as observed in *Verbascum, Buddleja*, saffron and other *Crocus* species [30,42,46–48].

4.2. A CCD2 enzyme catalyzes the biosynthesis of crocins in Crocosmia x crocosmiiflora

We found that a CCD that belongs to the CCD2 subfamily, named here as CroCCD2, which showed high similarity with the PhCCD2 from *F. hybrida* [28], catalyzes the reaction corresponding to the first step in the crocins pathway. This reaction renders crocetin dialdehyde as the first product. The remaining steps are catalyzed by aldehyde dehydrogenases, and glucosyltransferases that belong to different subfamilies in the plants studied [29,46,49,50]. The previously identified CCD2 enzymes, CsCCD2L and PhCCD2, recognize as substrate the carotenoid zeaxanthin. CroCCD2 recognized *in vivo* zeaxanthin as a substrate and its transient expression in *N. benthamiana* plants allowed the accumulation of crocins at levels comparable to the ones obtained when the saffron enzyme, CsCCD2L, was expressed. Previous studies using this virus-driven transient expression of CsCCD2L resulted in the production of crocins (~2 mg/g DW) at 13 dpi [add 31]. The levels obtained in this study were three times higher for CsCCD2L and twice as high for CroCCD2, most likely due to the collection of fully infected leaf tissue, which prevented dilution of the final product with uninfected tissue. These results demonstrate that this system is an effective platform for producing these important bioactive apocarotenoids in large quantities within a relatively short time.

4.3. Encapsulation of crocins improves their anti-inflammatory activities

The most abundant crocin in saffron, with 4 glucose molecules, is difficult to be absorbed into the systemic compartment following oral ingestion due to its strong water solubility, and weak lipophilicity [51]. Therefore, several studies have focused on developing nanocarriers to improve the bioavailability of crocins [52–54]. We found that crocins present in the polar extracts obtained from the flowers of *Crocosmia x crocosmiiflora* were not able to reverse the inflammatory effects induced by the treatment of RAW264.7 cells with LPS, suggesting that the highly glucosylated crocins present in the polar extract were not able to pass the cell membrane. Therefore, we decided to test the anti-inflammatory activity using exosomes and liposomes as carriers of crocins. Exosome-like particles derived from different plant species, as ginger or carrot, exhibit anti-inflammatory effects, showing their potential in biomedical applications [55]. In the other hand, liposomes are the most explored nanocarriers used in targeted drug delivery systems [56]. In the current study, exosomes obtained from *Crocosmia x crocosmiiflora* flowers were isolated, and liposomes containing crocins were obtained. Our results showed that both kind of nanocarriers, exosomes and crocin-containing liposomes, inhibited LPS-induced NO production and INOS expression and protein levels in RAW264.7 cells. In addition, both can reduce the expression of toxic mediators (NO, INOS, COX2), interferon IFN-β, pro-inflammatory cytokines (IL-1, IL-6, TNF-α, IL-1β) and anti-inflammatory cytokines (IL-10), in the LPS-induced RAW 264.7 cells. Previous studies have demonstrated that crocins modulate inflammatory pathways across various conditions. For instance, in a cirrhotic rat model of hepatocellular carcinoma, crocins downregulated NF-κB and COX2 [57]. Similarly, in ulcerative colitis, crocin treatment led to the suppression of NF-κB and COX2, along with pro-inflammatory cytokines such as TNF-α, IL-1β, and IL-6. which were also downregulated together with TNF-α, IL-1β, and IL-6 [58]. Crocetin exhibits its anti-inflammatory properties through a mechanism involving the inhibition of the MEK1/JNK/NF-κB/INOS pathway and activation of the Nrf2/HO-1 pathway. Notably, a direct crosstalk has been observed between the MEK1/JNK/NF-κB/INOS pathway and the Nrf2/HO-1 pathway in crocetin-treated cells, which is critical for the observed anti-inflammatory effects [59], where HO-1 plays a key link point in this crosstalk. Consequently, crocetin functions as a redox balance modulator, precisely orchestrating its anti-inflammatory and chemo-preventive effects through the regulation of the crosstalk between the Nrf2/HO-1 and NF-κB/INOS pathways.

5. Conclusions

Metabolic engineering represents nowadays a powerful approach for improving the production of bioactive secondary metabolites highly demanded by the industry. Among several strategies, this boost can be achieved through the introduction of novel metabolic pathways into heterologous host systems and subsequently optimizing them for *de novo* production. By overexpressing a unique CCD gene, crocins production can be achieved, effectively redirecting the carotenoid flux towards the synthesis of these metabolites. Here, we provide a CCD2 enzyme that

effectively converts zeaxanthin into crocins as an innovative way to create improved production systems to secure the global need for crocins as potent anti-inflammatory compounds. In addition, we demonstrate how biological activity of crocins could be improved by the vehiculation of these molecules in natural nanocarriers as exosomes, which can be directly generated from the natural sources, or by the generation of liposomes that effectively encapsulate and transport crocins. We will further explore the use of a viral vector as an effective platform for the obtention of crocins-rich containing exosomes for direct clinical applications.

Funding

This work was supported by grant PID2020–114761RB-I00 and PID2020–114691RB-I00 and PID2023–146418OB-I00 from the MCIN/AEI /10.13039/501,100,011,033. LGG is a participant of the CARNET network (RED2022–134,577-T) from the MCIN/AEI.

Ethical

This work was supported by grants PID2020–114761RB-I00 and PID2020–114691RB-I00 from the Ministerio de Ciencia, Innovación y Universidades (Spain) through the Agencia Estatal de Investigación.

CRediT authorship contribution statement

Lucía Morote: Methodology, Investigation. **Cristian Martínez Martínez Fajardo:** Investigation. **María Mondéjar López:** Investigation. **Elena Moreno-Gimenez:** Writing – review & editing, Supervision, Investigation. **Ángela Rubio-Moraga:** Methodology. **Olivia Costantina Demurtas:** Methodology. **Gianfranco Diretto:** Methodology. **Enrique Niza:** Writing – review & editing, Methodology. **Verónica Aragonés:** Methodology, Investigation. **Alberto López Jiménez:** Methodology, Formal analysis. **José-Antonio Daròs:** Supervision, Formal analysis. **Oussama Ahrazem:** Writing – review & editing, Supervision, Resources, Formal analysis. **Lourdes Gómez-Gómez:** Writing – review & editing, Writing – original draft, Supervision, Project administration, Conceptualization.

Declaration of competing interest

The authors declare that they have no conflicts of interest.

Acknowledgements

This work was supported by grants PID2020–114761RB-I00, PID2020–114691RB-I00 and PID2023–146418OB-I00 from the Ministerio de Ciencia, Innovación y Universidades (Spain) through the Agencia Estatal de Investigación. L.G-G is a participant of the CARNET network (RED2022–134577-T). J.-A.D., L.G-G and O.A. belong to the Associated Unit Tomafran (IB-UCLM and IBMCP-CISC-UPV). We appreciated the support of Drs Susana López-López and Mª José Martínez Díaz-Guerra (Fac. Medicine, UCLM).

Supplementary materials

Supplementary material associated with this article can be found, in the online version, at doi:10.1016/j.btre.2025.e00891.

Data availability

Data will be made available on request.

References

[1] M. Rodriguez-Concepcion, J. Avalos, M.L. Bonet, A. Boronat, L. Gomez-Gomez, D. Hornero-Mendez, M.C. Limon, A.J. Melendez-Martinez, B. Olmedilla-Alonso, A. Palou, J. Ribot, M.J. Rodrigo, L. Zacarias, C. Zhu, A global perspective on carotenoids: metabolism, biotechnology, and benefits for nutrition and health, Prog. Lipid Res. 70 (2018) 62–93.
[2] T. Sun, S. Rao, X. Zhou, L. Li, Plant carotenoids: recent advances and future perspectives, Mol. Hortic. 2 (1) (2022) 3.
[3] R. Caferri, Z. Guardini, R. Bassi, L. Dall'Osto, Assessing photoprotective functions of carotenoids in photosynthetic systems of plants and green algae, Meth. Enzymol. 674 (2022) 53–84.
[4] A. Alder, M. Jamil, M. Marzorati, M. Bruno, M. Vermathen, P. Bigler, S. Ghisla, H. Bouwmeester, P. Beyer, S. Al-Babili, The path from beta-carotene to carlactone, a strigolactone-like plant hormone, Sci. 335 (6074) (2012) 1348–1351.
[5] S.H. Schwartz, B.C. Tan, D.A. Gage, J.A. Zeevaart, D.R. McCarty, Specific oxidative cleavage of carotenoids by VP14 of maize, Sci. 276 (5320) (1997) 1872–1874.
[6] J.Y. Wang, I. Haider, M. Jamil, V. Fiorilli, Y. Saito, J. Mi, L. Baz, B.A. Kountche, K. P. Jia, X. Guo, A. Balakrishna, V.O. Ntui, B. Reinke, V. Volpe, T. Gojobori, I. Blilou, L. Lanfranco, P. Bonfante, S. Al-Babili, The apocarotenoid metabolite zaxinone regulates growth and strigolactone biosynthesis in rice, Nat. Commun. 10 (1) (2019) 810.
[7] N.E. Polyakov, A.I. Kruppa, T.V. Leshina, T.A. Konovalova, L.D. Kispert, Carotenoids as antioxidants: spin trapping EPR and optical study, Free Radic. Biol. Med. 31 (1) (2001) 43–52.
[8] W.S. Blaner, Chapter 5 - Vitamin A and provitamin A carotenoids, in: B.P. Marriott, D.F. Birt, V.A. Stallings, A.A. Yates (Eds.), Present Knowledge in Nutrition, 11th Edition, Academic Press, 2020, pp. 73–91.
[9] A.F.G. Cicero, A. Colletti, Effects of carotenoids on health: are all the same? results from clinical trials, Curr. Pharm. Des. 23 (17) (2017) 2422–2427.
[10] T. Maoka, Carotenoids as natural functional pigments, J. Nat. Med. 74 (1) (2020) 1–16.
[11] G. Sandmann, Diversity and evolution of carotenoid biosynthesis from prokaryotes to plants, Adv. Exp. Med. Biol. 1261 (2021) 79–94.
[12] X. Zheng, Y. Yang, S. Al-Babili, Exploring the diversity and regulation of apocarotenoid metabolic pathways in plants, Front. Plant Sci. 12 (2021).
[13] J.C. Moreno, J. Mi, Y. Alagoz, S. Al-Babili, Plant apocarotenoids: from retrograde signaling to interspecific communication, Plant J. 105 (2) (2021) 351–375.
[14] O. Ahrazem, L. Gomez-Gomez, M.J. Rodrigo, J. Avalos, M.C. Limon, Carotenoid cleavage oxygenases from microbes and photosynthetic organisms: features and functions, Int. J. Mol. Sci. 17 (11) (2016).
[15] S. Perveen, I.H. Sadler, R. Orfali, A.M. Al-Taweel, L. Murray, S.C. Fry, Montbresides A-D: antibacterial p-coumaroyl esters of a new sucrose-based tetrasaccharide from Crocosmia × crocosmiiflora (montbretia) flowers, Fitoterapia. 139 (2019) 104377.
[16] N. Nagamoto, H. Noguchi, A. Itokawa, K. Nakata, K. Namba, H. Nishimura, M. Matsui, M. Mizuno, Antitumor constituents from bulbs of Crocosmia crocosmiiflora, Planta Med. 54 (4) (1988) 305–307.
[17] Y. Asada, T. Ueoka, T. Furuya, Novel Acylated Saponins from Montbretia (Crocosmia crocosmiiflora). Isolation of Saponins and the Structures of Crocosmiosides A, B and H, Chem. Pharm. Bull. 37 (8) (1989) 2139–2146.
[18] S. Irmisch, S. Jancsik, M.M.S. Yuen, L.L. Madilao, J. Bohlmann, Biosynthesis of the anti-diabetic metabolite montbretin A: glucosylation of the central intermediate mini-MbA, The Plant J. 100 (5) (2019) 879–891.
[19] S. Ootani, K. Hayashi, Further search for water soluble carotenoids in yellow flowers of several plants, Res. Inst. Evolut. Biol. Sci. Rep. 1 (1982) 6.
[20] L. Morote, M. Lobato-Gómez, O. Ahrazem, J. Argandoña, B. Olmedilla-Alonso, A. J. López-Jiménez, G. Diretto, R. Cuciniello, P. Bergamo, S. Frusciante, E. Niza, Á. Rubio-Moraga, S. Crispi, A. Granell, L. Gómez-Gómez, Crocins-rich tomato extracts showed enhanced protective effects in vitro, J. Funct. Foods. 101 (2023) 105432.
[21] S. Bastani, V. Vahedian, M. Rashidi, A. Mir, S. Mirzaei, I. Alipourfard, F. Pouremamali, H. Nejabati, J. kadkhoda, N.F. Maroufi, M. Akbarzadeh, An evaluation on potential anti-oxidant and anti-inflammatory effects of Crocin, Biomed. Pharmacother. 153 (2022) 113297.
[22] L. Pourmousavi, R.H. Asadi, F. Zehsaz, R.P. Jadidi, Potential therapeutic effects of crocin, Naunyn. Schmiedebergs. Arch. Pharmacol. 397 (10) (2024) 7395–7420.
[23] O. Ahrazem, G. Diretto, J. Argandona, A. Rubio-Moraga, J.M. Julve, D. Orzaez, A. Granell, L. Gomez-Gomez, Evolutionarily distinct carotenoid cleavage dioxygenases are responsible for crocetin production in Buddleja davidii, J. Exp. Bot. 68 (16) (2017) 14.
[24] L. Gómez-Gómez, L. Morote, C.M. Fajardo, Á. Rubio-Moraga, S. Frusciante, G. Diretto, O. Ahrazem, Engineering the production of crocins and picrocrocin in heterologous plant systems, Ind. Crops. Prod. 194 (2023) 116283.
[25] S. Frusciante, G. Diretto, M. Bruno, P. Ferrante, M. Pietrella, A. Prado-Cabrero, A. Rubio-Moraga, P. Beyer, L. Gomez-Gomez, S. Al-Babili, G. Giuliano, Novel carotenoid cleavage dioxygenase catalyzes the first dedicated step in saffron crocin biosynthesis, Proc. Natl. Acad. Sci. U S A 111 (33) (2014) 12246–12251.
[26] O. Ahrazem, A. Rubio-Moraga, J. Berman, T. Capell, P. Christou, C. Zhu, L. Gomez-Gomez, The carotenoid cleavage dioxygenase CCD2 catalysing the synthesis of crocetin in spring crocuses and saffron is a plastidial enzyme, New Phytol. 209 (2) (2016) 13.
[27] X. Zheng, J. Mi, A. Balakrishna, K.X. Liew, A. Ablazov, R. Sougrat, S. Al-Babili, Gardenia carotenoid cleavage dioxygenase 4a is an efficient tool for biotechnological production of crocins in green and non-green plant tissues, Plant Biotechnol. J. 20 (11) (2022) 2202–2216.

[28] Q. Fang, Y. Li, B. Liu, X. Meng, Z. Yang, S. Yang, T. Bao, S. Kimani, X. Gao, L. Wang, Cloning and functional characterization of a carotenoid cleavage dioxygenase 2 gene in safranal and crocin biosynthesis from Freesia hybrida, Plant Physiol. Biochem. 154 (2020) 439–450.
[29] Z. Xu, X. Pu, R. Gao, O.C. Demurtas, S.J. Fleck, M. Richter, C. He, A. Ji, W. Sun, J. Kong, K. Hu, F. Ren, J. Song, Z. Wang, T. Gao, C. Xiong, H. Yu, T. Xin, V. A. Albert, G. Giuliano, S. Chen, J. Song, Tandem gene duplications drive divergent evolution of caffeine and crocin biosynthetic pathways in plants, BMC. Biol. 18 (1) (2020) 63.
[30] L. Morote, Á. Rubio-Moraga, A.J. López Jiménez, V. Aragonés, G. Diretto, O. C. Dermutas, S. Frusciante, O. Ahrazem, J.-A. Daròs, L. Gómez-Gómez, Verbascum species as a new source of saffron apocarotenoids and molecular tools for the biotechnological production of crocins and picrocrocin, The Plant J. 118 (2024) 14.
[31] M. Martí, G. Diretto, V. Aragonés, S. Frusciante, O. Ahrazem, L. Gómez-Gómez, J.-A. Daròs, Efficient production of saffron crocins and picrocrocin in Nicotiana benthamiana using a virus-driven system, Metab. Eng. 61 (2020) 238–250.
[32] D. Subha, K. Harshnii, K.G. Madhikiruba, M. Nandhini, K.S. Tamilselvi, Plant derived exosome- like Nanovesicles: an updated overview, Plant Nano Biol. 3 (2023) 100022.
[33] C.Martínez Fajardo, L. Morote, E. Moreno-Giménez, S. López-López, Á. Rubio-Moraga, M.J.M. Díaz-Guerra, G. Diretto, A.J. López Jiménez, O. Ahrazem, L. Gómez-Gómez, Exosome-like nanoparticles from Arbutus unedo L. mitigate LPS-induced inflammation via JAK-STAT inactivation, Food Funct. 15(22) (2024) 11280–11290.
[34] B.D. Isailović, I.T. Kostić, A. Zvonar, V.B. Đorđević, M. Gašperlin, V.A. Nedović, B. M. Bugarski, Resveratrol loaded liposomes produced by different techniques, Innov. Food Sci. Emerg. Technol. 19 (2013) 181–189.
[35] M. Etxebeste-Mitxeltorena, E. Niza, C.M. Fajardo, C. Gil, L. Gómez-Gómez, A. Martinez, O. Ahrazem, Neuroprotective properties of exosomes and chitosan nanoparticles of Tomafran, a bioengineered tomato enriched in crocins, Nat. Prod. Bioprospect. 14 (1) (2024) 9.
[36] R. Newton, Molecular mechanisms of glucocorticoid action: what is important? Thorax. 55 (7) (2000) 603–613.
[37] L. Gomez-Gomez, G. Diretto, O. Ahrazem, S. Al-Babili, Determination of in vitro and in vivo activities of plant carotenoid cleavage oxygenases, Methods Mol. Biol. 2083 (2020) 63–74.
[38] J. Xu, N. Liu, E. Polemiti, L. Garcia-Mondragon, J. Tang, X. Liu, T. Lett, L. Yu, M. M. Nöthen, J. Feng, C. Yu, A. Marquand, G. Schumann, H. Walter, A. Heinz, M. Ralser, S. Twardziok, N. Vaidya, E. Serin, M. Jentsch, E. Hitchen, R. Eils, U.-H. Taron, T. Schütz, K. Schepanski, J. Banks, T. Banaschewski, K. Jansone, N. Christmann, A. Meyer-Lindenberg, H. Tost, N. Holz, E. Schwarz, A. Stringaris, M. Neidhart, F. Nees, S. Siehl, O.A. Andreassen, L.T. Westlye, D. van der Meer, S. Fernandez, R. Kjelkenes, H. Ask, M. Rapp, M. Tschorn, S.J. Böttger, G. Novarino, L. Marr, M. Slater, G.F. Viapiana, F.E. Orosa, J. Gallego, A. Pastor, A. Forstner, P. Hoffmann, M.M. Nöthen, A.J. Forstner, I. Claus, A. Miller, S. Heilmann-Heimbach, P. Sommer, M. Boye, J. Wilbertz, K. Schmitt, V. Jirsa, S. Petkoski, S. Pitel, L. Otten, A.-P. Athanasiadis, C. Pearmund, B. Spanlang, E. Alvarez, M. Sanchez, A. Giner, S. Hese, P. Renner, T. Jia, Y. Gong, Y. Xia, X. Chang, V. Calhoun, J. Liu, P. Thompson, N. Clinton, S. Desrivieres, A.H. Young, B. Stahl, G. Ogoh, M.C. the environ, effects of urban living environments on mental health in adults, Nat. Med. 29 (6) (2023) 1456–1467.
[39] M. Hashemzaei, C. Mamoulakis, K. Tsarouhas, G. Georgiadis, G. Lazopoulos, A. Tsatsakis, E. Shojaei Asrami, R. Rezaee, Crocin: a fighter against inflammation and pain, Food Chem. Toxicol. 143 (2020) 111521.
[40] G.-L. Xu, G. Li, H.-P. Ma, H. Zhong, F. Liu, G.-Z. Ao, Preventive effect of crocin in inflamed animals and in LPS-challenged RAW 264.7 Cells, J. Agric. Food Chem. 57 (18) (2009) 8325–8330.
[41] Z. Maqbool, M.S. Arshad, A. Ali, A. Aziz, W. Khalid, M.F. Afzal, S.P. Bangar, M. Addi, C. Hano, J.M. Lorenzo, Potential role of phytochemical extract from saffron in development of functional foods and protection of brain-related disorders, Oxid. Med. Cell Longev. 2022 (2022) 6480590.
[42] A.R. Moraga, J.L. Rambla, O. Ahrazem, A. Granell, L. Gomez-Gomez, Metabolite and target transcript analyses during crocus sativus stigma development, Phytochem. 70 (8) (2009) 1009–1016.
[43] S.R. Sommano, P. Suppakittpaisarn, K. Sringarm, T. Junmahasathien, W. Ruksiriwanich, Recovery of crocins from floral tissue of gardenia jasminoides ellis, Front. Nutr. 7 (2020).
[44] T. Abu-Izneid, A. Rauf, A.A. Khalil, A. Olatunde, A. Khalid, F.A. Alhumaydhi, A.S. M. Aljohani, M. Sahab Uddin, M. Heydari, M. Khayrullin, M.A. Shariati, A. O. Aremu, A. Alafnan, K.R.R. Rengasamy, Nutritional and health beneficial properties of saffron (Crocus sativus L): a comprehensive review, Crit. Rev. Food Sci. Nutr. 62 (10) (2022) 2683–2706.
[45] A. Rubio Moraga, O. Ahrazem, J.L. Rambla, A. Granell, L.Gomez Gomez, Crocins with high levels of sugar conjugation contribute to the yellow colours of early-spring flowering crocus tepals, PLoS. One. 8(9) (2013) e71946.
[46] G. Diretto, A.J. López-Jiménez, O. Ahrazem, S. Frusciante, J. Song, Á. Rubio-Moraga, L. Gómez-Gómez, Identification and characterization of apocarotenoid modifiers and carotenogenic enzymes for biosynthesis of crocins in Buddleja davidii flowers, J. Exp. Bot. 72 (8) (2021) 3200–3218.
[47] O. Ahrazem, J. Argandona, A. Fiore, C. Aguado, R. Lujan, A. Rubio-Moraga, M. Marro, C. Araujo-Andrade, P. Loza-Alvarez, G. Diretto, L. Gomez-Gomez, Transcriptome analysis in tissue sectors with contrasting crocins accumulation provides novel insights into apocarotenoid biosynthesis and regulation during chromoplast biogenesis, Sci. Rep. 8 (1) (2018) 2843.
[48] O. Ahrazem, A. Rubio-Moraga, J. Argandona-Picazo, R. Castillo, L. Gomez-Gomez, Intron retention and rhythmic diel pattern regulation of carotenoid cleavage dioxygenase 2 during crocetin biosynthesis in saffron, Plant Mol. Biol. 91 (3) (2016) 355–374.
[49] A.J. López-Jimenez, S. Frusciante, E. Niza, O. Ahrazem, Á. Rubio-Moraga, G. Diretto, L. Gómez-Gómez, A new glycosyltransferase enzyme from family 91, UGT91P3, Is responsible for the final Glucosylation step of Crocins in saffron (Crocus sativus L.), Int. J. Mol. Sci. 22 (16) (2021).
[50] L. Gomez-Gomez, L.F. Pacios, A. Diaz-Perales, M. Garrido-Arandia, J. Argandona, A. Rubio-Moraga, O. Ahrazem, Expression and interaction analysis among saffron ALDHs and Crocetin Dialdehyde, Int. J. Mol. Sci. 19 (5) (2018).
[51] Y.-N. Song, Y. Wang, Y.-H. Zheng, T.-L. Liu, C. Zhang, Crocins: a comprehensive review of structural characteristics, pharmacokinetics and therapeutic effects, Fitoterapia. 153 (2021) 104969.
[52] S. Tavasoli, Z. Borjizadeh, A. Anvar, H. Ahari, S. Moradi, S.M. Jafari, Crocin-loaded nanocarriers; approaches and applications, current opinion in food, Sci. 54 (2023) 101099.
[53] Y. Pian, Y. Hao, Y. Guo, S. Wu, S. Tang, J. Li, X. Lu, X. Sun, Z. Tan, T. Zhu, Y. Tang, D. Xu, H. Hu, Exploration of using α-crocin for drug encapsulation and delivery, J. Drug Deliv. Sci. Technol. 106 (2025) 106716.
[54] Z. Khaksari, F. Mehri, M.H. Abdolvahab, M.A. Manavi, M.H.F. Nasab, A. Karbasi, M. Baeeri, A. Ranjbar, Crocin and Nano-Crocin Mitigate Paraquat Hepatotoxicity by modulating expression of genes involved in oxidative stress and inflammation, Pharm. Nanotechnol. (2025).
[55] J. Mondal, S. Pillarisetti, V. Junnuthula, S.S. Surwase, S.R. Hwang, I.K. Park, Y. K. Lee, Extracellular vesicles and exosome-like nanovesicles as pioneering oral drug delivery systems, Front. Bioeng. Biotechnol. 11 (2023) 1307878.
[56] H. Nsairat, D. Khater, U. Sayed, F. Odeh, A. Al Bawab, W. Alshaer, Liposomes: structure, composition, types, and clinical applications, Heliyon. 8 (5) (2022) e09394.
[57] B. Awad, A.A. Hamza, A. Al-Maktoum, S. Al-Salam, A. Amin, Combining crocin and sorafenib improves their tumor-inhibiting effects in a rat model of Diethylnitrosamine-induced Cirrhotic-hepatocellular carcinoma, Cancers. 15 (16) (2023) 4063.
[58] G.A. Albalawi, M.Z. Albalawi, K.T. Alsubaie, A.Z. Albalawi, M.A.F. Elewa, K. S. Hashem, M.M.H. Al-Gayyar, Curative effects of crocin in ulcerative colitis via modulating apoptosis and inflammation, Int. Immunopharmacol. 118 (2023) 110138.
[59] Y.L. Wen, Z. He, D.X. Hou, S. Qin, Crocetin exerts its anti-inflammatory property in LPS-Induced RAW264.7 cells potentially via modulation on the crosstalk between MEK1/JNK/NF-κB/iNOS Pathway and Nrf2/HO-1 Pathway, Oxid. Med. Cell Longev. 2021 (2021) 6631929.